

# The Quantitative Analysis of Fluorocarbon Polymer Finishes on Wool by FT-IR Spectroscopy

JEFFREY S. CHURCH\* and DAVID J. EVANS

Commonwealth Scientific Industrial Research Organisation, Division of Wool Technology, P.O. Box 21, Belmont, Victoria 3216, Australia

## SYNOPSIS

Two contrasting infrared spectroscopic techniques, Attenuated Total Reflectance (ATR) and PhotoAcoustic Spectroscopy (PAS), have been investigated as means for the determination of fluorocarbon polymer finishes on wool fabric. Based on the experimental conditions used, the results of the PAS method are more characteristic of the bulk sample, while the ATR results are more surface specific. Linear calibrations between polymer add-on, as determined by total fluorine analysis, and the absorbance of the C—F stretching bands of the normalized spectral data were obtained for a typical commercial fluorocarbon polymer. The correlation obtained for the PAS method was found to be significantly better than that of the ATR method. The lower limit of detection of fluorocarbon polymers on wool using the PAS technique was 0.25% on the weight of the wool (oww). In contrast, fluorocarbon polymer add-ons as low as 0.125% oww (approximating monolayer coverage) could be analyzed using the ATR method. At high levels of add-on, the ATR calibration deviated from linearity. This can be attributed to the distribution of fluorocarbon polymer on the surface of the fiber, in particular, the build up of polymer on the cuticle cell edge regions. The quantitative methods developed are used to help access the effects of wear and the subsequent heating of fluorocarbon polymer-treated fabric samples. © 1995 John Wiley & Sons, Inc.

## INTRODUCTION

Stain repellent treatments that impart oil and water repellency to fabrics have become important finishes for textiles in recent years.<sup>1,2</sup> These finishes consist of coating the surface of the fiber with a thin layer of polymer containing perfluoroalkyl side chains. The pendant fluoroalkyl chains orientate at the fiber-air interface and, after curing, yield a surface that resembles a perfluorocarbon polymer. This confers on the fiber surface the low attractive force characteristic of these polymers that is responsible for high oil and water repellency. The use of fluorocarbon polymer based stain repellent finishes for wool has been reviewed by Lewis.<sup>3</sup> Wool goods suitable for application of fluorocarbon polymers include

career apparel, protective clothing, upholstery, and carpets.<sup>3,4</sup>

A number of techniques have been used to characterize fluorocarbon polymers on the surfaces of textiles. These include wetting measurements,<sup>5,6</sup> infrared spectroscopy,<sup>7</sup> and x-ray photoelectron spectroscopy.<sup>5,6</sup> Total fluorine analysis by wet chemical analysis is generally used for quantitative analysis of fluorocarbon polymers on textiles.<sup>8</sup> Combustion of the samples in an oxygen atmosphere followed by analysis of total fluorine, measured in solution as fluoride, is required because of the resistance of the C—F bond to chemical attack. Due to the nature of this type of analysis, no specific information is obtained regarding the component of the fluorocarbon polymer that is actually on the surface of the fiber.

The surface-sensitive technique of Attenuated Total Reflectance (ATR) infrared spectroscopy has previously been used for the detection of fluorocarbon polymers on rayon-ramie blends<sup>7</sup> but has not been investigated as a tool for quantitative analysis.

\* To whom correspondence should be addressed.

The application of PhotoAcoustic (PA) spectroscopy to the analysis of polymer finishes on textiles was first reported by Yang and co-workers.<sup>9</sup> Their work on cotton yarns treated with various sizing agents demonstrated that the PA technique was an ideal method for obtaining information on the chemical nature of the near surface. The ATR and PA techniques differ significantly in their sampling characteristics. The ATR technique provides chemical information only from the surface area in intimate contact with the Internal Reflecting Element (IRE). In contrast, the PA signal generally originates from much deeper within the sample and is not influenced by the texture of the sample.

In order to chemically access the changes in the fluorocarbon polymer following wear and subsequent heating of treated fabric samples, it was important to establish quantitative methods for both the surface and bulk polymer. This article describes the application of ATR and PA FT-IR spectroscopies coupled with total fluorine analysis to the quantitative determination of fluorocarbon polymer finishes on treated wool fabric samples.

## EXPERIMENTAL

### Materials

A light weight ( $190 \text{ gm}^{-2}$ ) plain-weave fabric of  $21 \mu\text{m}$  wool was used for all experiments. Prior to use the fabric was scoured with a nonionic surfactant (Lissapol TN450, ICI), adjusted to pH 4–5 with acetic acid and then rinsed thoroughly with distilled water.

The fluorocarbon polymer, Oleophobol S (Ciba Geigy), is a proprietary product described as a per-fluoroalkyl polymer emulsion with a slightly cationic nature and was used as received from the supplier.

### Treatment of Wool with Fluorocarbon Polymer

Samples of wool fabric containing a known amount of fluorocarbon polymer on the mass of wool were prepared as follows. An aliquot of fluorocarbon polymer emulsion sufficient to just wet out the fabric sample was dispersed in aqueous acetone (1 : 1). The solution was then spread over the fabric with the aid of a spatula to give an even application of polymer on the surface. The sample was then fixed to a metal frame and turned end over end until dry. Wool samples were then cured at  $140^\circ\text{C}$  for 5 min and conditioned at 65% RH and  $20^\circ\text{C}$  before analysis. All application levels of fluorocarbon polymer

discussed in this work are for solid polymer on the weight of wool (oww).

### Oil Repellency

The AATCC hydrocarbon resistance test method 118–1992,<sup>10</sup> with a scale from 0 (no oil repellency) to 8 (extremely high oil repellency), was used.

### Water Repellency

Water repellency is normally accessed by the AATCC spray test method,<sup>11</sup> but due to the small size of the abraded samples and in order to maintain consistency, a static water drop test was used. This test is analogous to the oil repellency test and determines the resistance of the treated fabric to wetting by aqueous liquids. Drops of eight different water–isopropanol mixtures varying from 10% isopropanol (water repellency rating 1) to 80% isopropanol (rating 8) in increments of 10% isopropanol are placed on the fabric's surface. The extent of surface wetting using this range of liquids is then determined visually. This test provides a rough guide of the aqueous stain resistance in that generally the higher the water repellency rating, the better the finished fabric's resistance to staining by aqueous-based substances.

### Abrasion

Abrasion tests were carried out with a Martindale abrasion tester.<sup>12</sup> Test specimens of both the treated and untreated fabrics were subjected to 500 abrasion rubs.

### Fluorine Analysis of Fluorocarbon Polymer-Treated Wool

The fluorine content of fluorocarbon polymer-treated wool was determined by combustion analysis (Schöniger oxidation) of 10 to 20 mg samples cut from different areas of the treated fabric. Combustion was performed in a 500 mL quartz oxidation flask (Heraeus) fitted with a quartz stopper and a platinum wire carrier (PSP Industries model No. CO 11). The flask was flushed with ultrahigh purity oxygen (CIG) immediately before the burning of the sample. Deionized water ( $\leq 18 \text{ M}\Omega \text{ cm}$ , 10.00 mL) was used as the absorbing solution. The solution was analyzed for fluoride using a Dionex 4500i ion chromatograph equipped with a Dionex IonPac AS4A column. The mobile phase was 5.0 mM sodium tetraborate at a flow rate of 2 mL/min.

Strongly retained ions such as sulfate were flushed from the column by using a step gradient to 50 mM sodium tetraborate after 2 min. The method was linear over the range 0.01 to 10 ppm of fluoride. Recovery of fluoride from combustion of a sample of 2,4 dinitro-5-fluoroaniline was 99%. Analyses were performed in duplicate.

### Secondary Electron Imaging and Elemental Analysis

Secondary electron imaging and Energy Dispersive X-ray (EDX) analysis were carried out using a Hitachi model S-4100 cold field emission scanning electron microscope fitted with a Noran Voyager EDX spectrometer. Prior to imaging, the samples were coated with 2 nm of chromium using a Dynavac Xenosput 2000. Images were obtained using a 1.0 kV accelerating voltage and 5 mm working distance. EDX analyses were carried out using a 15 kV accelerating voltage on samples that were coated with 150–200 Å of carbon. Elemental maps for carbon, oxygen, fluorine, and sulfur were collected from areas typically of  $20 \times 20 \mu\text{m}$  at a 128 pixel  $\times$  128 pixel resolution using a dwell time of 0.1 s.

### Spectroscopic Analysis

Infrared spectra were recorded using a Perkin-Elmer System 2000 Fourier transform infrared spectrometer equipped with a narrow-band MCT detector. Data acquisition and manipulation was carried out with PE-Grams/2000 version 2.0 (Galactic Industries Corp., Salem, NH). Interferograms were collected as double sided, unidirectional, and a medium apodization function was applied.

The ATR spectra were collected at a resolution of  $4 \text{ cm}^{-1}$  using a SPECAC model 11900 variable angle accessory fitted with a ZnSe IRE held at  $45^\circ$  to the incident beam. Each spectrum was the result of co-adding 32 scans collected at an optical velocity of  $2.0 \text{ cm/s}$ . Two  $10 \times 40 \text{ mm}$  coupons were cut from each of the fabric samples to be analyzed. The quantitative results reported are based on the spectral average of all four sides of the two sample coupons.

The PA spectra were recorded at a resolution of  $8 \text{ cm}^{-1}$  using a MTEC model 200 accessory. Ultra-high purity helium (CIG) was used as the coupling gas, and a carbon black film (MTEC) was used as a reference sample. Photoacoustic spectra with the optimum signal-to-noise ratio were obtained by co-adding 512 scans collected at an optical velocity of  $0.05 \text{ cm/s}$ . Samples for analysis by PA spectroscopy were cut from the fabric using a 6 mm diameter

punch. By stacking four fabric disks in the sample holder, sufficient space was left between the sample and the cell window for the generation of the photoacoustic signal.

## RESULTS AND DISCUSSION

Prior to the development of a quantitative method it is best to characterize the individual components comprising the system to be analyzed. This is particularly important when the analyte is a commercial product of which little is known and the substrate is a complex material. Aside from identifying specific spectral features that will allow for the identification and subsequent quantification of the components of interest, the information obtained should help provide a clear understanding of the limitations of the analytical methods developed.

### Characterization of the Fluorocarbon Polymer

The infrared transmission spectrum obtained from a thin film of the fluorocarbon is shown as Figure 1(A). The most intense bands in this spectrum are observed at  $1202$  and  $1150 \text{ cm}^{-1}$  and can be assigned

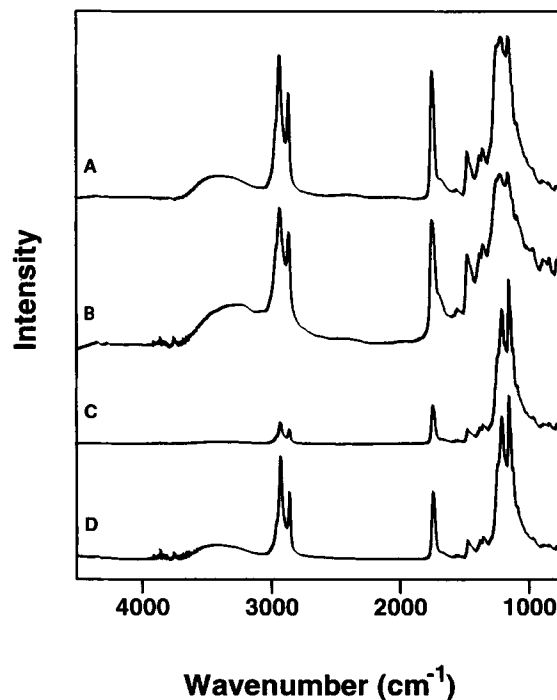


**Figure 1** The infrared spectra obtained from a cured sample of Oleophobol S by (A) transmission, (B) PAS, (C) ATR, and (D) ATR after correction for variations in effective sample thickness.

to the  $\text{CF}_2$  symmetric and asymmetric stretching vibrations.<sup>13</sup> Weaker shoulders associated with the  $\text{CF}_3$  symmetric and degenerate asymmetric stretching modes are observed at 1135 and 1236  $\text{cm}^{-1}$ , respectively.<sup>14</sup> The spectrum also exhibits a strong carbonyl absorption at 1738  $\text{cm}^{-1}$ . The intense symmetric and asymmetric stretching vibrations of the  $\text{CH}_2$  groups are observed at 2926 and 2855  $\text{cm}^{-1}$ , respectively, while the corresponding deformational modes appear as a much weaker absorption at 1468  $\text{cm}^{-1}$ .<sup>13</sup> It is most probable that these  $\text{CH}_2$  groups form part of the backbone of the polymer and that the carbonyl group is part of an ester linkage connecting the  $\text{CF}_2$  chains to the backbone. The weak absorption at 1346  $\text{cm}^{-1}$  can be assigned to a C—H bending vibration also associated with the polymer backbone.<sup>13</sup> A weak broad hydrogen-bonded hydroxyl stretching vibration is observed centred near 3367  $\text{cm}^{-1}$ .<sup>13</sup> This hydroxyl stretching vibration can most probably be associated with the glycol type surfactant that can be isolated from the commercial product by centrifugation ( $12,000 \times g$  for 3 h). Also, this absorption band is not observed in spectra obtained from the most dense polymer fractions isolated in this manner. Based on the analysis of the infrared data, the repeat unit of the polymer most likely consists of a perfluoroalkyl chain connected to a polyvinyl acetate backbone through an ester linkage. Commercial polymers of this type have been disclosed.<sup>1</sup>

#### Application of ATR and PAS to Fluorocarbon Polymer Analysis

The ATR signal strength is related to the depth of penetration,  $d_p$ , of the incident radiation into the sample. The sampling depth varies with wavelength,  $\lambda$ , according to the equation:

$$d_p = \lambda / n_1 2\pi (\sin^2 \theta - n_{21}^2)^{1/2}$$

where  $d_p$  is defined as the depth into the sample at which the electric field amplitude decreases to a value of  $1/e$  of that at the surface,  $\theta$  is the angle of incidence, and  $n_{21}$  is the ratio of the refractive indices of the rarer,  $n_2$ , to the denser,  $n_1$ , medium.<sup>15</sup> Using this equation, values of 1.55 and 2.42 for the refractive indices of wool<sup>16</sup> and ZnSe, respectively, and an angle of incidence of  $45^\circ$ , the  $d_p$  at 1200  $\text{cm}^{-1}$  (C—F stretching region) is calculated to be on the order of 1.8  $\mu\text{m}$ .

The ATR spectrum obtained from a film of the fluorocarbon polymer cured on an aluminium foil substrate is shown as Figure 1(C). By comparison,

the relative intensities of the peaks of the ATR spectrum are significantly different from those of the transmission spectrum obtained from the same material. These differences are partially due to the wavelength dependence of the depth of penetration of the incident radiation into the sample as mentioned above. ATR spectra can be corrected for this variance in effective pathlength by applying the equation:

$$\text{Abs}_{\text{corrected}} = \text{Abs}_{\text{measured}} / (\lambda - c),$$

where  $c$  is a scale factor chosen such that the resultant ATR spectrum is in the best agreement with the transmission spectra obtained from the sample. The corrected spectrum obtained by using the maximum possible value for  $c$  is shown as Figure 1(D). This spectrum more closely resembles the transmission spectrum [1(A)] than the uncorrected spectrum [1(C)]; however, significant intensity differences are still apparent. These differences are most likely due to the fact that the optical constants of the sample and IRE are not true constants, but vary with wavelength.

The intensity of the PA signal generated by a sample is related to its optical and thermal properties. Rosencwaig<sup>17</sup> has classified materials as either optically opaque or transparent and thermally thick or thin, depending on the relationship between their absorption coefficients and thermal diffusion lengths. Textile materials such as wool and cotton are generally thermally thick and optically thin; thus, a major contribution to their PA spectra is obtained from the first thermal diffusion length,  $\mu_{\text{th}}$ . The thermal diffusion length of a material is related to the modulation frequency of the incident radiation,  $\omega$ , by the following equation:

$$\mu_{\text{th}} = (2k / \rho c \omega)^{1/2}$$

where  $k$  is thermal conductivity,  $\rho$  is density, and  $c$  is heat capacity. The angular modulation frequency for a rapid scanning interferometer of the type used in this experiment is related to optical velocity,  $V$ , by the relationship:

$$\omega = 2\pi\nu V$$

where  $\nu$  is the frequency in wave numbers of the incident radiation. Based on these equations, and values of  $k = 5.4 \times 10^{-2} \text{ W/mK}$ ,<sup>18</sup>  $c = 1.36 \text{ J/gK}$ ,<sup>16</sup> and  $\rho = 1.32 \text{ kg/m}^3$ ,<sup>16</sup> a  $\mu_{\text{th}}$  of 10.5  $\mu\text{m}$  at 1200  $\text{cm}^{-1}$  can be calculated for an interferometer operating at an optical velocity of 0.05  $\text{cm/s}$ . Considering the 21

$\mu\text{m}$  average diameter of the wool fibers used in this work, PAS data collected under these conditions should be representative of the bulk of the sample. For a scan speed of 0.5 cm/s, the value for  $\mu_{\text{th}}$  calculated is 3.3  $\mu\text{m}$ , which is nearly twice the depth of penetration of the ATR experiment.

The photoacoustic spectrum obtained at an optical velocity of 0.05 cm/s from a bulk sample of the cured polymer is shown as Figure 1(B). By comparison, this spectrum can be seen to be very similar to the transmission spectrum. This similarity confirms the validity of the long thermal diffusion length calculated at very low modulation frequency, which in turn, results in a spectrum that is typical of the bulk.

### Characterization of Fluorocarbon Polymer-Treated Wool

The secondary electron images obtained from typical fibers in the fabric sample before and after treatment with 1% oww fluorocarbon polymer are shown as Figure 2(A) and (B), respectively. The image obtained from the untreated sample clearly exhibits the sharp-edged cuticle structure typical of  $\alpha$ -keratin fibers. In the image obtained from the fluorocarbon polymer-treated sample, the fiber appears to be completely covered with the polymer, with thicker deposition at the scale edges.

EDX maps obtained from the treated fibers revealed that the cuticle surface was composed mainly of carbon, with minor amounts of evenly distributed oxygen and sulfur. The absence of fluorine reflects the thinness of the fluorocarbon polymer coating in this area. In contrast, the areas at the cuticle edges were found to be composed mostly of fluorine, with a minor amount of carbon being detected. No sulfur or oxygen could be detected in this area. Considering the sample density and data collection parameters, it can be approximated that the EDX signal is being generated from an onion-shaped volume extending 1.5 to 2  $\mu\text{m}$  below the surface. These results are in agreement with the polymer distribution implied from the secondary electron images. The film thickness and uniform coverage of the cuticle surfaces suggested by these results indicate that the polymer film would be quite suitable for near surface FT-IR techniques such as ATR and PA spectroscopies.

The 1800 to 1000  $\text{cm}^{-1}$  region of the ATR spectra obtained from wool fabric treated with 1% oww fluorocarbon polymer and untreated wool fabric are shown as Figure 3(A) and (B), respectively. From a comparison of these spectra, it is apparent that the quantitation of the fluorocarbon polymer could

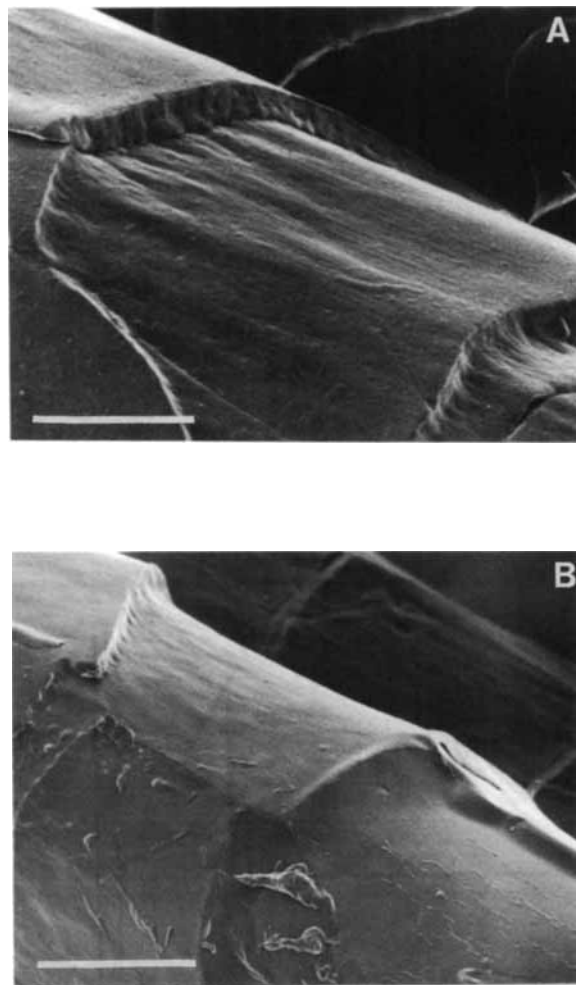


**Figure 2** The secondary electron image obtained using a 1 kV accelerating voltage from a typical wool fiber in (A) an untreated wool fabric sample (bar, 4.50  $\mu\text{m}$ ) and (B) a wool fabric sample treated with 1% oww Oleophobol S (bar, 6.00  $\mu\text{m}$ ).

be possible using the C=O stretching vibration of the fluorocarbon polymer observed at 1741  $\text{cm}^{-1}$ . This vibrational mode appears to be an ideal candidate, as it is well resolved from spectral features arising from the wool substrate. Alternatively, the strong C—F stretching vibrations (1202 and 1150  $\text{cm}^{-1}$ ) could be used; however, these bands overlap with the amide III region of the wool spectrum.

### Preparation of Fluorocarbon Polymer Standards

As add-ons for fluorocarbon polymer treatments are typically less than 1.0% oww, a series of standard samples were prepared comprising 0.125, 0.25, 0.5, 0.75, and 1.0% oww Oleophobol S. Initially, treated fabric samples were prepared by padding the fabrics

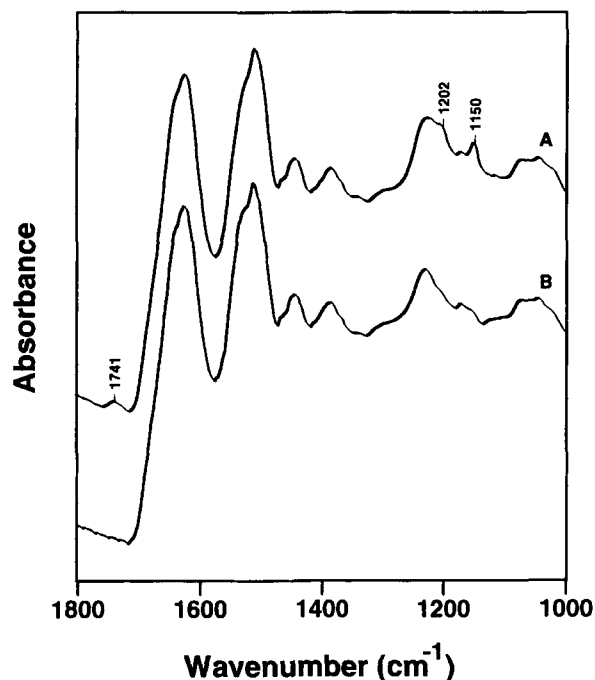


**Figure 3** The ATR spectra of the 1800 to 1000  $\text{cm}^{-1}$  region of (A) wool treated with 1% oww Oleophobol S and (B) untreated wool.

with an isopropanol/water mixture of the fluorocarbon polymer using a laboratory pad mangle and drying at room temperature. However, as previously observed by McNeil,<sup>19</sup> the correlation of the total fluorine content with the nominal add-on was found to be poor. In general, the fluorine content found by Schöniger analysis was found to be greater than the theoretical value, and subsequent work showed that this was due to rapid adsorption of fluorocarbon polymer onto the surface of the fabric at ambient temperature.<sup>20</sup>

A second method for preparing fabric samples with known amounts of fluorocarbon polymer was developed in which the desired weight of fluorocarbon polymer was dispersed in a volume of isopropanol/water just sufficient to wet out the fabric sample. The fabric samples prepared in this manner were then allowed to dry laying flat in a Petri dish before curing. The total fluorine content determined for the samples prepared in this manner were found to be in excellent agreement with the theoretical. For example, the total fluorine content of the 1% oww fluorocarbon polymer-treated fabric was determined to be  $2.89 \pm 0.3$  mg fluorine/g wool, which is in very good agreement with the theoretical value of 2.97 mg fluorine/g wool based on the fluorine content of the polymer.

The ATR analysis of these samples revealed large face-to-back deviations in the intensities of both the 1741 and 1202  $\text{cm}^{-1}$  peaks relative to the Amide II peak. In contrast, the analysis of the same face of two adjacently sampled ATR coupons were very reproducible. These variations are probably due to the wicking of the polymer dispersion to the upper face of the fabric during drying. The face to back differences in the polymer surface distribution were minimized (reduced by a factor of 4) by using the tumble drying technique described in the experimental section of this article.

Oil and water repellency measurements were used to determine if the fabric treatments were satisfactory. Oil repellency ratings of 0 and 8 were obtained for untreated and treated fabric samples, respectively. The static water drop method gave ratings of 1 and 8 for untreated and treated fabric samples, respectively. The results of the static water drop method may appear misleading, as they tend to indicate that the natural water repellency of untreated wool is relatively poor. However, it has been shown that the observed critical surface tension of untreated wool when measured against water/alcohol mixtures gives much lower values than when measured with nonpolar liquids. It has been suggested that this is due to adsorption of alcohol on the surface of the fiber.<sup>21</sup> The water repellencies determined using this test can, therefore, only be used as a relative guide of a fabric's ability to resist wetting by polar liquids.

### Quantitative Analysis

As discussed above, the carbonyl stretching vibration of the fluorocarbon polymer observed at 1741  $\text{cm}^{-1}$  appears to be the best choice for the development of a quantitative method. Initial attempts to quantitate the fluorocarbon polymer were made using this peak. After normalising the ATR spectra on the amide II band at 1511  $\text{cm}^{-1}$ , the intensity of the 1741  $\text{cm}^{-1}$  absorption was plotted as a function of fluorocarbon polymer as determined by total fluorine analysis. The resulting plot was nonlinear, and exhibited a very large degree of scatter, making it unuseable for quantitation. A similar plot using the integrated area of the carbonyl absorption was also found to be unacceptable. Several reasons could be put forth for this lack of correlation, including interference from water vapor lines in this spectral region and contamination with typical lipid matter picked up during handling of the samples. It is also worthwhile noting that the intensity of the carbonyl

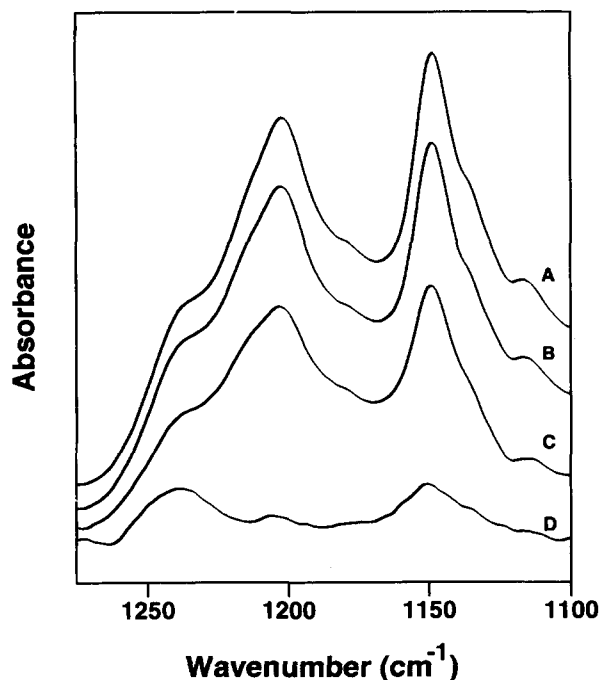


**Figure 4** The 1275 to 1100  $\text{cm}^{-1}$  region of the spectra resulting from the subtraction of the ATR spectra obtained from (A) a 1% oww, (B) 0.75%, (C) 0.5%, and (D) 0.25% Oleophobol S-treated fabric samples and the untreated fabric sample.

band in the uncorrected ATR spectrum [Fig. 1(C)] is very weak.

The other spectral feature identified that could be used for the analysis was the strong C—F stretching fundamentals observed at 1202 and 1150  $\text{cm}^{-1}$ . As depicted in Figure 3(A), the 1150  $\text{cm}^{-1}$  band is the only feature in this region of the raw data that could possibly be used. Due to its weak intensity at low levels of add-on and its overlap with the amide III region of the wool spectrum, the calibration plot obtained was also not acceptable.

An alternative technique for producing a viable calibration plot that involved the isolation of the C—F stretching region of the fluorocarbon polymer from the wool spectrum by spectral subtraction was developed. After normalization, the spectra obtained from the treated fabric samples were subtracted from the spectrum obtained from a sample of the parent fabric using a scale factor of unity. A series of spectra resembling that of the fluorocarbon polymer were obtained. The 1275 to 1100  $\text{cm}^{-1}$  region of this series of spectra are shown as Figure 4.

Linear correlation plots using either the intensity (1150 or 1202  $\text{cm}^{-1}$ ) or area (1275–1100  $\text{cm}^{-1}$ ) of this absorption data were successful with the integrated area of the C—F stretching vibration pro-

ducing slightly better results. A plot of the average integrated C—F stretching absorption area determined by ATR as a function of fluorocarbon polymer determined by total fluorine analysis for the series of standard samples is shown as Figure 5. If a least squares regression is carried out with all of the data points, a linear correlation with an  $r^2$  value of 0.91 is obtained. The equation for this line, labeled A in Figure 5, is  $\text{Abs}_{\text{C-F}} = 2.52 \times \text{Conc}[\text{F}] + 1.03$ . The major problem with this line of fit is the very high Y-intercept value of 1.03 Abs units. A much better fit as well as a more meaningful calibration can be obtained if the data point corresponding to the 1% add-on is removed from the data set. If this is done, the line labeled B in Figure 5 is obtained. The equation for this line is  $\text{Abs}_{\text{C-F}} = 3.67 \times \text{Conc}[\text{F}] + 0.07$  and the  $r^2$  value is 0.95. These results indicate that the ATR method is not linear at add-ons above 0.75% oww. This is most likely due to the build up of fluorocarbon polymer in the cuticle cell edge region at high levels of add-on, as observed from the secondary electron images obtained from the sample [Fig. 2(B)]. Polymer build-up in this area would not be as readily detected by the ATR technique, because it is not in intimate contact with the IRE.

The carbonyl absorption of the fluorocarbon polymer was not observed as a resolved feature in

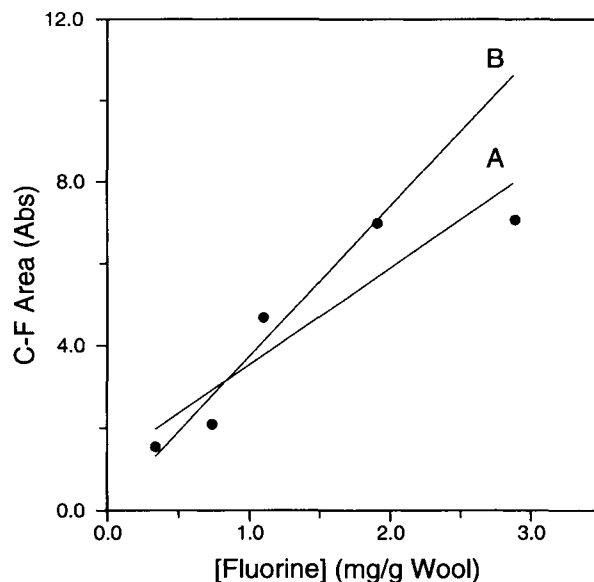


**Figure 5** A plot of integrated C—F stretching area as determined by ATR spectroscopy as a function of fluorocarbon polymer determined by total fluorine analysis for a series of Oleophobol S-treated fabric samples: (A) least squares fit for add-ons from 0.125 to 1.0% Oleophobol S, (B) least squares fit for add-ons from 0.125 to 0.75% Oleophobol S.

the PA spectra obtained from the treated samples at the slow scan speeds. This is due to the photoacoustic saturation of the amide I and II regions. Furthermore, this saturation prevented the use of the amide II band for normalization. Use of the amide A band centred near  $3300\text{ cm}^{-1}$  was also not desirable, as possible differences in fiber regain could cause intensity differences in this spectral region. However, due to the high level of uniformity in the sample preparation, and data acquisition, the spectra obtained were found to be of very consistent intensity in the amide III region. A method of spectral subtraction was adopted that involved the adjustment of the scale factor until a spectrum in excellent agreement with that obtained from the neat cured polymer was obtained. In all cases, the final resulting scale factors were close to unity. The resulting spectra were carefully analyzed to insure that there were no artefacts in the spectral regions of interest due to saturation or subtraction effects. The  $1275$  to  $1100\text{ cm}^{-1}$  region of the series of spectra generated in this manner from the standard samples are shown as Figure 6.

A calibration plot based on the average integrated C—F stretching absorption area determined by PAS for the series of standard samples is shown as Figure

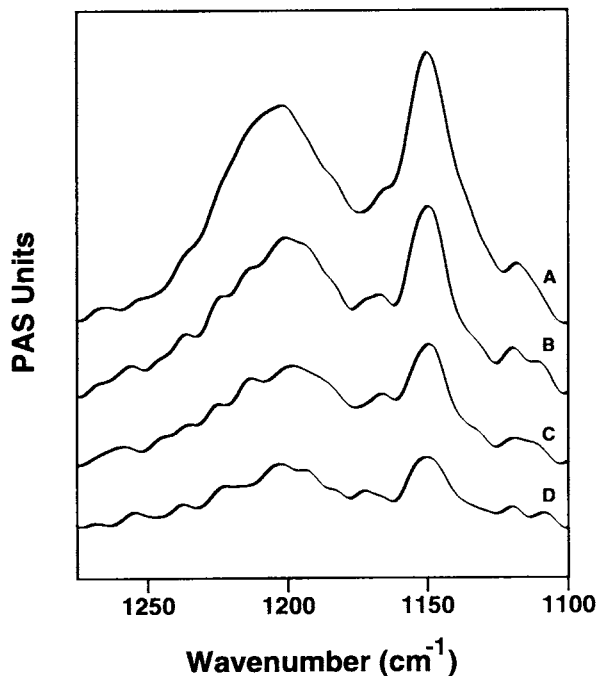


**Figure 6** The  $1275$  to  $1100\text{ cm}^{-1}$  region of the spectra resulting from the subtraction of the PA spectra obtained from (A) a 1% oww, (B) 0.75%, (C) 0.5%, and (D) 0.25% Oleophobol S-treated fabric samples and the untreated fabric sample.

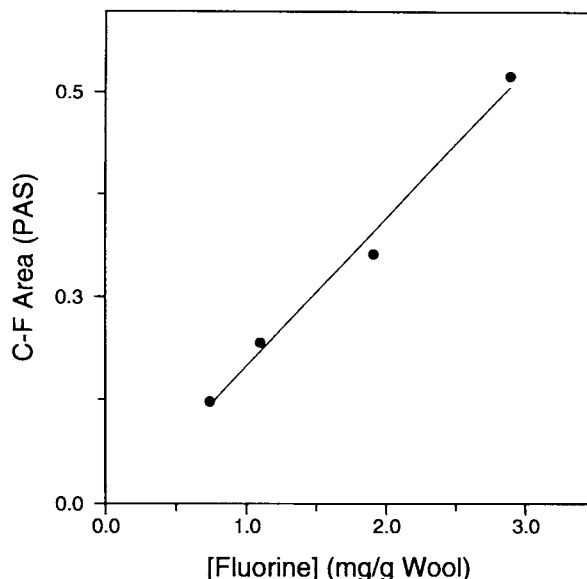


**Figure 7** A plot of integrated C—F stretching area as determined by PAS as a function of fluorocarbon polymer determined by total fluorine analysis for a series of Oleophobol S-treated fabric samples.

7. The equation obtained for the line of best fit for this data is  $\text{Abs}_{\text{C-F}} = 0.18 \times \text{Conc}[\text{F}] - 0.02$ . The  $r^2$  value obtained for this linear correlation is 0.99. No fluorocarbon polymer could be detected on the 0.125% oww-treated sample by PA spectroscopy. An attempt to improve the sensitivity of the PA method was made by collecting the data at faster optical velocities. As the PA signal would originate from a shallower depth within the sample, the contribution from the surface fluorocarbon polymer would be greater. It was found, however, that even at surface penetrations as shallow as  $2\text{ }\mu\text{m}$ , any gains derived from an increased fluorocarbon polymer signal component were out weighed by loss in signal to noise ratio.

#### Quantitation of Unknown Samples

In order to access the usefulness of these quantitative methods, they were used in combination with repellency and total fluorine measurements to monitor the treatment and wear of an actual sample. As can be seen from the results given in Table I, the initial measurements made on a fabric sample treated with 1% oww Oleophobol S are very consistent with those expected.

After abrasion with 500 rubs, both the oil and water repellencies of the sample drop to the level of the untreated fabric. The examination of the abraded sample in the scanning electron microscope



**Table I** The Results of the Analysis of a 1% oww Oleophobol S-Treated Sample before and after Abrasion and Subsequent Heat Treatment

Sample Treatment	Repellency		mg [F]/g Wool ( $\pm 0.3$ )		
	Oil [1]	Water <sup>a</sup>	Total <sup>b</sup>	ATR	PAS
Untreated	0	1	0	—	—
1% Oleophobol S	8	8	2.9	2.9 <sup>c</sup>	3.0
Abraded 500 rubs	0	1	2.9	< 0.1	2.7
Abraded 500 rubs, heated	8	8	2.9	0.2	2.7

<sup>a</sup> Static water drop test method.

<sup>b</sup> As determined by Schöniger oxidation.

<sup>c</sup> Calculated using ATR calibration line "A," all other values calculated using line "B."

revealed that the fluorocarbon polymer as well as most of the cuticles in the contact area of the fabric were removed, exposing untreated wool. Significant amounts of this debris was observed embedded within the bulk of the fibrous structure of the fabric. This is why the fluorocarbon polymer is virtually undetectable by the ATR method. The total fluorine content of the abraded sample as determined by Schöniger oxidation was identical to that of the un-abraded-treated sample and, correspondingly, the value determined by the PA method was only slightly less.

It is well known that heat treatment of worn fluorocarbon polymer-treated fabric samples restores both water and oil repellencies.<sup>6</sup> As evident from Table II, this is what is observed for the abraded sample after heat treatment at 105°C for 5 min. The ATR results indicate that a film significantly greater than a monolayer has been reformed over the contact surface even though no such film could be detected from the secondary electron images or EDX spectra obtained from the sample. As expected, the heat treatment did not effect the fluorine content, as determined by the Schöniger oxidation and PA methods. It is worthwhile noting, however, that the C—F stretching absorptions observed in the PA spectra obtained from the heat-treated sample were much sharper and well defined compared to those observed in the spectra obtained from the sample after abrasion. This probably indicates an improvement in the uniformity of the polymer coating of the fibers.

## CONCLUSIONS

Fluorocarbon polymer finishes on wool fabric can be quantitated using the FT-IR techniques of ATR and PA spectroscopies. Linear correlation between

polymer add-on and infrared signal were obtained for both techniques with the fit being significantly better for the PA data. The interpretation of the results as well as the limitations of the two methods can be understood in terms of the differences in the sampling characteristics of the two techniques.

The application of these new quantitative methods to an abraded and subsequently heat-treated sample has demonstrated their usefulness as well as their contrasting nature. Total fluorine analysis and PA data do not correlate with oil or water repellency, as they are bulk measurements. The ATR data does correlate because of its surface specificity. A combination of techniques is, therefore, required to fully understand the effect of abrasion on fluorocarbon polymer-treated fabric and the mechanism whereby a heat treatment restores the repellency.

The authors recognize the support of the Australian wool growers who fund research and development through the International Wool Secretariat. The technical assistance of D. Robinson and A. L. Wilde is also appreciated.

## REFERENCES

1. D. Lammermann, *Melliand Textilber*, **72**, 949 (1991).
2. P. Otto, *Melliand Textilber*, **72**, 378 (1991).
3. J. Lewis, *Wool Sci. Rev.*, **48**, 42 (1974); Part 2, **49**, 47 (1974).
4. P. E. Ingham, *Aust. Text.*, **9**(6), 27 (1989).
5. Y. Sato, T. Wakida, S. Tokino, S. Niu, M. Ueda, H. Mizushima, and S. Takekoshi, *Text. Res. J.*, **64**, 316 (1994).
6. T. Wakida, H. Li, Y. Sato, H. Kawamura, M. Ueda, H. Mizushima, and S. Takekoshi, *J. Soc. Dyers Colour*, **109**, 292 (1993).
7. R. V. Flor and M. J. Prager, *J. Text. Inst.*, **73**, 138 (1982).

8. S. Mitzner, in *Analytical Methods for a Textile Laboratory*, 2nd Ed., AATCC Monograph No. 3., J. W. Earver, Ed. American Association of Textile Chemists and Colorists, Research Triangle Park, 1968, pp. 153–155.
9. Q. C. Yang, T. J. Ellis, R. R. Breese, and W. G. Fateley, *Appl. Spectrosc.*, **41**, 889 (1987).
10. AATCC Test Method 118–1992, American Association of Textile Chemists and Colorists, Research Triangle Park, 1994.
11. AATCC Test Method 22–1989, American Association of Textile Chemists and Colorists, Research Triangle Park, 1994.
12. AS 200.2.25, Standards Australia, North Sydney, 1990.
13. L. J. Bellamy, *The Infrared Spectra of Complex Molecules*, Wiley, New York, 1958, pp. 15, 20, 99, 100, 179, 180, 328–33.
14. H. W. Thompson and R. B. Temple, *J. Chem. Soc., Lond.*, 1432 (1948).
15. N. J. Harrick, *Internal Reflection Spectroscopy*, John Wiley and Sons, New York, 1967, p. 30.
16. H. R. Mauersberger, Ed., *Matthew's Textile Fibers: Their Physical, Microscopical and Chemical Properties*, J. Wiley and Sons, New York, 1947, pp. 38, 46, 60.
17. A. Rosencwaig, *Photoacoustics and Photoacoustic Spectroscopy*, J. Wiley and Sons, New York, 1980, pp. 271–273.
18. W. E. Morton and J. W. S. Hearle, *Physical Properties of Textile Fibres*, 2nd Ed., The Textile Institute, Manchester, 1975, p. 591.
19. S. J. McNeil, *Text. Res. J.*, **60**, 244 (1990).
20. D. J. Evans, unpublished results.
21. B. O. Bateup, J. R. Cook, H. D. Feldman, and B. E. Fleischfresser, *Text. Res. J.*, **46**, 720 (1976).

Received November 28, 1994

Accepted February 25, 1995